Scientific Research Publishing

Open Journal of Geology, 2025, 15(3), 174-197
https://www.scirp.org/journal/ojg
ISSN Online: 2161-7589
ISSN Print: 2161-7570

Portrait of an Impact Strewn Field—Thermoclastic Ricochet Track: Eocene-Oligocene Transition (EOT), Jordan, Arabian Plate

Werner Schneider[1], Elias Salameh[2]

[1]Formerly Braunschweig Technical University, Braunschweig, Germany
[2]University of Jordan, Amman, Jordan
Email: salameli@ju.edu.jo

How to cite this paper: Schneider, W. and Salameh, E. (2025) Portrait of an Impact Strewn Field—Thermoclastic Ricochet Track: Eocene-Oligocene Transition (EOT), Jordan, Arabian Plate. *Open Journal of Geology*, **15**, 174-197.
https://doi.org/10.4236/ojg.2025.153008

Received: February 27, 2025
Accepted: March 23, 2025
Published: March 26, 2025

Abstract

Almost coevally with worldwide impact events, immediately at the beginning of the Eocene-Oligocene Transformation (EOT), (34.0 - 33.5 Ma), the Jordanian Platform and adjacent areas underwent an Impact Strewnfield/Ricochet-Scenery along a W/NW-striking ~400 km long strip, connected with triggered basalt magmatism (B1 - B3) and relating to the initial Red Sea Opening (34 Ma). The members of the Impact Ensemble expose along the "Fireline" a broad spectrum of characteristic impact structures (crater, ring structures, irregular structures) exhibiting thermo-clastic deformation ranging from low temperature to pyroxenite-sanidine hornfels facies of the Maastrichtian to Eocene target rocks (carbonate-, chert deposits), chert melt (~1400˚C: Jebel Waqf as Suwwan) and many mineral neoformations up to >1100˚C. Careful lithostratigraphic reviewing (including nannoplankton, and pelagic foraminifers) in the remote NE, near the Jordanian/Iraqi border area, and modern δ^{13}C- and δ^{18}C-isotope data of high resolution allow detailed age interpretation of impacting, triggered basalt magmatismus (B1 - B3) and lithofacies change from pelagic "Greenhouse"-carbonate rocks to oxygene-deficient bituminous baryte-bearing marls during stepwise microfauna extinction and high disturbance ("Cosmic Winter"-Environment: 34.0 - 33.9 Ma = 100 kyr). After the EOT, the lithofacies changed abruptly above a significant unconformity to glauconite-bearing mixed siliciclastics during the Early Oligocene Glacial Maximum (EOGM 33.5 - 33.0 Ma), followed by recovered lithofacies and microfauna under rising temperature. The subvolcanic precursors of the Red Sea-Opening (*i.e.* Sinai) penetrated the Arabian Shield by sills and dikes (44.42 - 41.34 Ma) and provided a restricted magma volume up to a surface near "highstand-level", to be impact-triggered and to cause locally restricted outpourings (B1 - B3) or merely basaltic crater seams and jets without

outflow. The major plateau basalt outpourings/harrats (B4 - B6) across the Arabian Shield took place during Oligocene-Miocene B. to the Pleistocene, directed by plate tectonic forces in connection with the Red Sea-rifting and the collision of the Arabian with the Eurasian Plates.

Keywords

Volcanism, Impacting Affect Sedimentology, Mineralogy, Cosmic Winter, Jordanian Platform

1. Introduction

The impulse for focussing on the Eocene-Oligocene Transformation (EOT) of the Jordanian Platform (**Figure 1**) relates to a former publication in OJG [1], also dealing with the EOT in the Subhercynian Basin, N Germany, where principally similar geologic phenomena and driving forces became relevant:

A prominent unconformity, a significant paleobotanic (dinocysts) and lithofacies change, paleogeographic resetting combined with outstanding high-impact activity and climate change of global scale throughout the EOT (~34 Ma) are evidently there. Thereby, several tektite strewnfields ([2]-[4] meet major impacts [5] as the meteorite craters Popigai, Siberia (~100 km Ø. 35.7 ± 0.2 Ma), Chesapeake, N America (~85 km Ø, ~35.5 ± 0.2 Ma), and Azuara, Spain (~30 - 40 km Ø, EOT) [6].

After the Paleocene-Neocene Temperature Maximum (PETM [7]: ~56 Ma) precursors of the EOT-events (change of plate motion around 42 - 40 Ma [8], **Figure 2**), initial Red Sea-sub-volcanism [9], **Figure 3**: ~44 - 41 Ma) and additional early impact events since ~38 Ma [4] were introduced to the stepwise mass extinction of foraminifers and nannoplankton [10]-[12]).

Extensive impacting and increasing rift- and plateau basalt-volcanism [9] [13]-[15] caused an abrupt climate change through the EOT time-span from "Green House" to "Ice House" conditions ("Cosmic Winter"); the extinction of the foraminifer family Hantkeninidae defines the Eocene-Oligocene Boundary (EOB) within the EOT [11] [12]. However, the complex interplay of pelagic microfauna and $\delta^{18}0$, $\delta^{13}C$-data at different investigation sites led to a twofold way of the EOB-definition: 33.9 Ma [16]: GTS 2012) and 33.7 Ma [17], CK 95), by that providing the basic analytical data for the processes during the EOT on the Arabian Plate [12] (**Figure 4**).

Accordingly, the monotonous pelagic Paleogene carbonate -chert deposition still exposing the Hantkeninida Family, ended abruptly in Jordan at the EOT-onset overlain with the basalt flows B1 - B3. The unconformity located between B3, 6 - 20 m thick paleosol and the overlying Oligocene glauconitic mixed clastics, comprise the EOB (~33.7 Ma), [13]-[15], **Figure 5**).

The ~100 - 150 m thick B1 - B3 outpourings, each covered by ~5 m thick paleosols and "clays", merely encountered by drilling (Hunting Tech. Services Ltd., London), play a key role in the analysis of this subtle E0T-zone of Jordan, since

the younger outcropping plateau basalt effusions B4 - B6 definitely overlie the Oligocene clastic in the area of Dahikiya, E Azraq Basin (Figure 5).

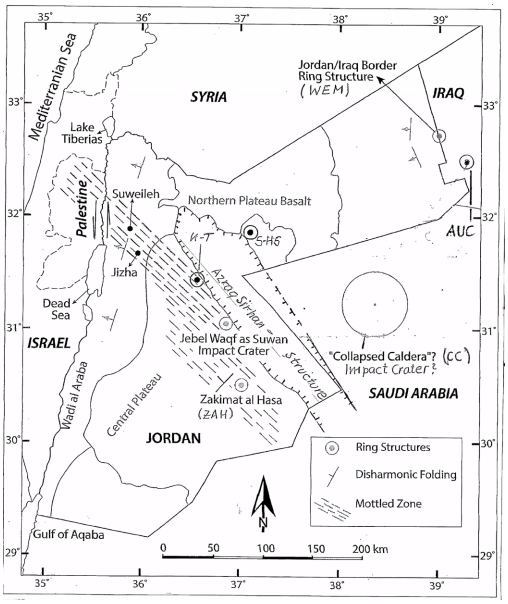

Figure 1. Verified and Suspicious impact structures and Ricochet track across Jordan and adjacent areas. Kh-T: between Qasr Kharana and Qasr Tuba, S-H5: between As Safra and pumping station H5, WEM: Wadi el Murbak.

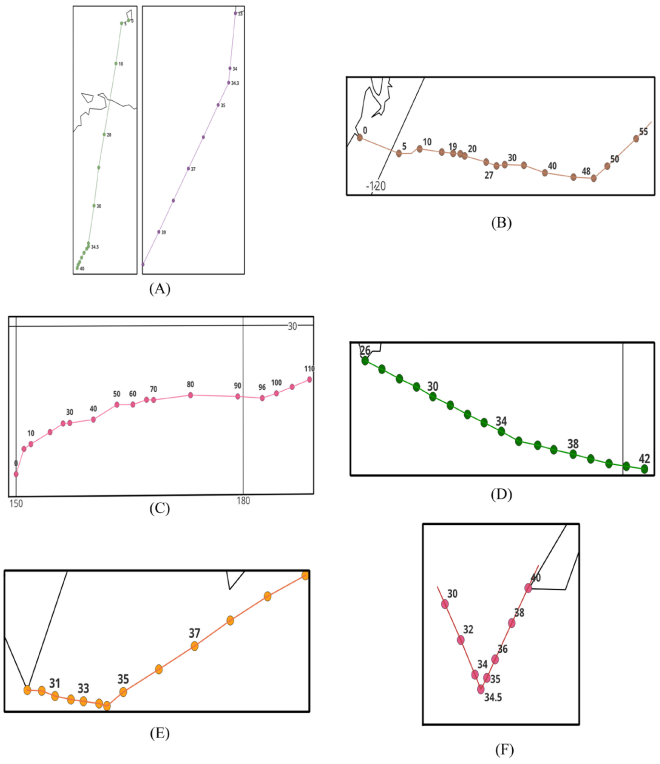

Figure 2. Change of plate motion (direction, velocity) in global scale throughout the Eocene-Oligocene Transition (EOT): (A) New Guinea, (B) N America, (C) Marianen, (D) Hawai, (E) Japan, (F) Banda. Arc, Popigai [8].

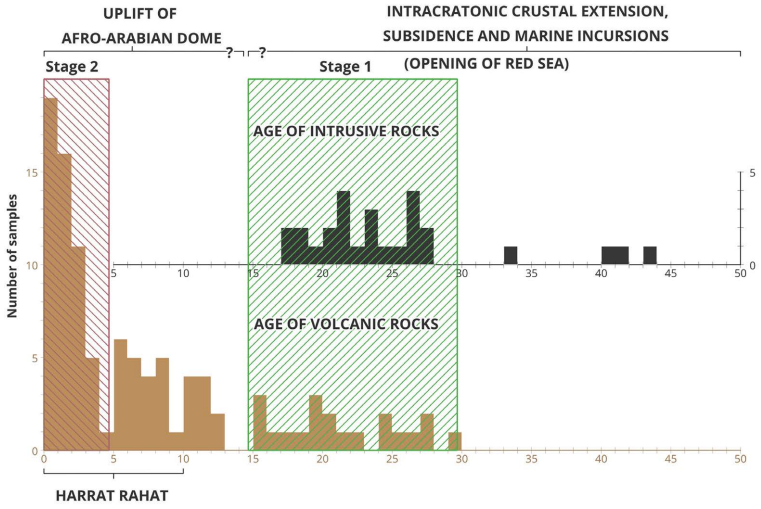

Figure 3. Intrusive precursors (44, 42 - 41, 34 Ma), [9] and magmatic stages [1] [2] of the Red Sea-opening since ~30 Ma [9]. B1 - B3 of Jordan relates to the early EOT, B4 - B6 meets the time-span Miocene to Early Pleistocene and the Saudi Arabian harrats as well.

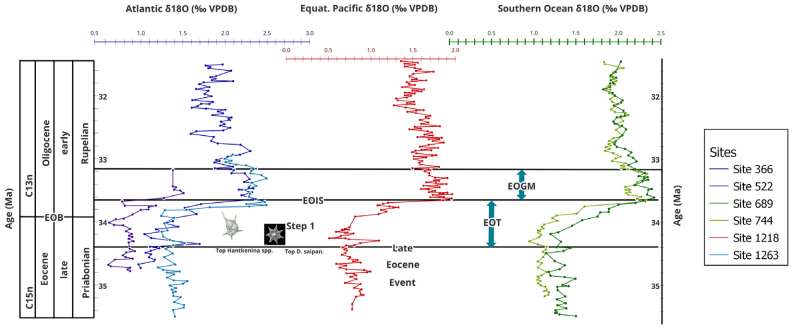

Figure 4. $\delta^{18}0$- excursions in the Equatorial Pacific and S Ocean through the EOT: EOB: Eocene-Oligocene boundary, EOT: Eocene-Oligocene Transition, EOIS: Earliest Oligocene oxygene isotope step, EOGM: Early Oligocene Glacial Maximum [12].

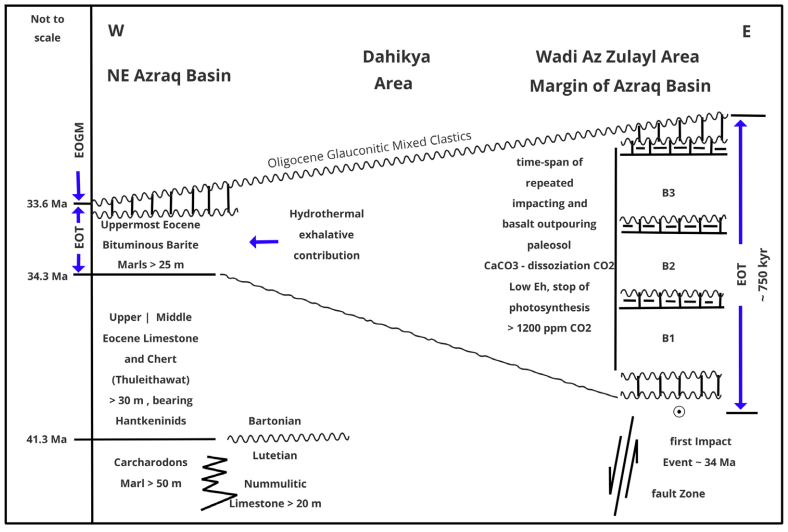

Figure 5. Lithostratigraphy through the EOT in NE Jordan including the early plateau basalt-outpourings B1 - B3 drilled in the Wadi as Zulayl area [13]-[15].

The Jordanian Plateau basalts (B_4 - B_6) cover ~11.000 km^2 and present only a small area of the huge outpourings between the Damascus Basin, Syria via NE Jordan, Saudi Arabia to Yemen (~180.000 km^2) effused from uppermost Oligocene to Early Pleistocene [9]-[14] [18] (**Figure 6**).

The basalt magma ascended along NW-striking fault systems that relate to the beginning Red Sea-rifting [9] [18] [19], Dead Sea-Jordan Valley rifting [13] [20], and the Miocene upheaval of the Arabian Shield [9] [18] [21].

The interest in the complex interplay of impacting, volcanism, and Red Sea-rifting was enhanced, in Jordan, by the discovery of the meteorite crater of Jebel Waqf as Suwwan, E Jordan in 2005 [22]-[24], which was strengthened by additional impact-suspicious ring structures and structural anomalies in adjacent areas including an unidentified large crater, in the NW of Saudi Arabia (~60 km Ø, **Figure 1**), and an Impact-Ricochet track extending from SE Jordan into Palestine [25]-[27], **Figure 1**.

All of them are identified as post-uppermost Eocene and own an identical lithostratigraphic position across the study area. So they are part of the EOT-zone as do the early basalt effusions B1 - B3 (**Figure 4**, **Figure 5**).

Thus, the Arabian Plate obviously exhibits an ENSEMBLE MEMBER in the record of the global EOT-Scenery [11] [12].

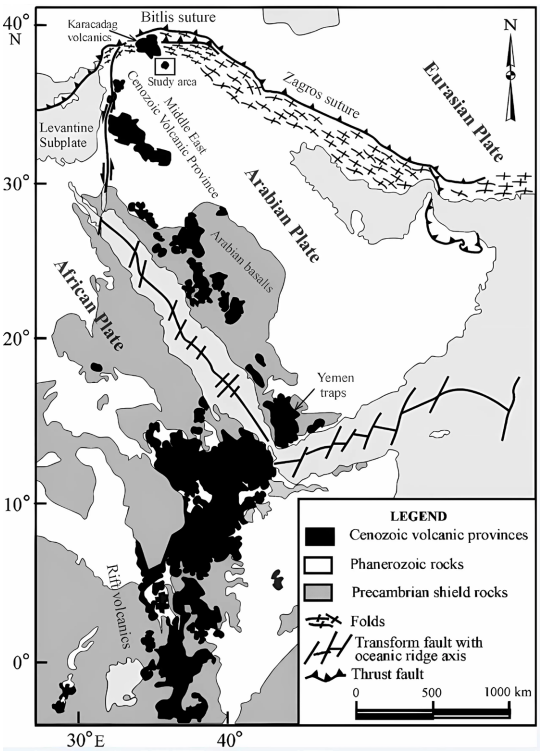

Figure 6. Occurrence of the Near/Middle East Plateau basalt-harrats extending across Yemen-Saudi Arabia-NE Jordan-Syria on the SW Arabian Plate accompanying the Red Sea-rifting [9].

2. Methodology Applied to the Target Area-Lithology

The WNW-extending study area located between the border triple junction Jordan-Iraq-Saudi Arabia (Jebel Aneiza) and Palestine (**Figure 1**) with the exception of the

Neogene plateau basalts is mainly built up of Late Cretaceous-Paleogene interbedded carbonate-chert series underlain by Early Cretaceous to Cenomanian Kurnub siliciclastics [13]-[15] (**Figure 5**).

During our first revisit of Jebel Waqf as Suwwan in 2005, formerly interpreted as "cryptovolcanic" structure [15] [34], the following impact features were verified [22]-[24]:

- Two types of shatter cones (**Figure 7**).
- Highly sheared chert breccia bearing tiny unidentified crystals of high refractive index (stishovite?) (**Figure 8**).
- Isolated angular chert fragments (ejecta!) sticking in carbonate ejecta by replacement (above ~900˚C!): "impact chess square" (**Figure 9**).

(A) (B)

Figure 7. Two types of shatter cones, Jebel Waqf as Suwwan [22] [26]. Note shearing and brecciation in micro-scale (B).

Figure 8. Highly brecciated and sheared chert, Jebel Waqf as Suwwan [22] [26].

- Silica bombs (originally chert, Kurnub sandstone) showing fluidal textures and impacts of small particles (arrow) under high viscosity, note also mm-thick surface layer! (Figure 10).

Microscopic studies of ejecta (quartz grains, SiO_2-glass) evidence:

- Planar deformation features (PDF) (Figure 11).

Figure 12 shows Plates of pseudohexagonal β-tridymite showing typical further recrystallisation to chalcedony, opal, quartz.

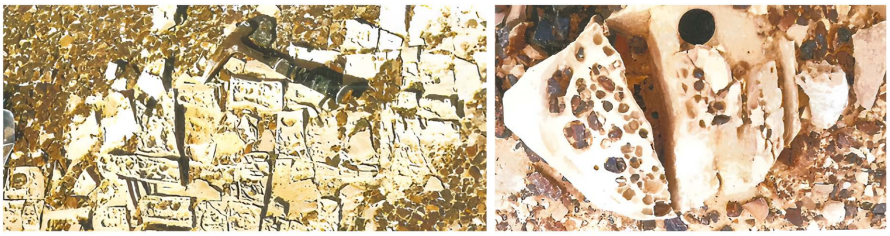

(A) (B)

Figure 9. "Rounded" chert and Kurnub-sandstone fragments still sticking in carbonate fall-out breccias caused by partial replacement ($CaC0_3$—replacement dissociation at ~900˚C), Jebel Waqf as Suwwan [22] [26].

(A) (B)

Figure 10. Chert bombs more or less totally melted (~1400˚C) exposing fluidal textures. Note little impacts of solid particles (arrow in (B)), Jebel Waqf as Suwwan [22] [26].

Figure 11. Four lattice plane Planar Deformation Features (PDF) in a quartz grain of Kurnub sandstone from clastic fall-out; thin section, Jebel Waqf as Suwwan [22] [26].

- The complete **regressive** recrystallisation-stages of the $Si0_2$-melt (**Figure 13**): Stalk-like pseudomorps of β-cristobalite recrystallized from α-cristobalite. (**Figure 14**): "Ballen-Structure" generated by the transformation of α- to β-cristobalite as result of volume reduction (~7%).

Most of these features were later reconfirmed during profound crater analysis [23] [24].

The so-called "Mottled Zone", ~50 km in width and ~180 km in length, striking from SE Jordan to Palestine, is built up with more or less bituminous Maastrichtian-Paleocene carbonate-chert series, which underwent thermo-cataclysm under

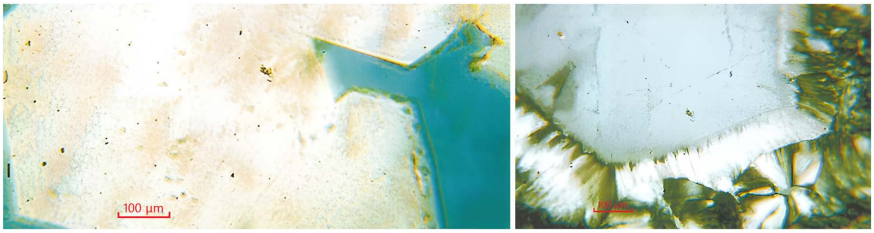

Figure 12. Plates of pseudo-hexagonal β-tridymite showing typical triplets; recrystallization to chalcedony. Note "rim cement". Originally melted Kurnub sandstone from the Central Uplift of Jebel Waqf as Suwwan [26], thin section, X-Nicols.

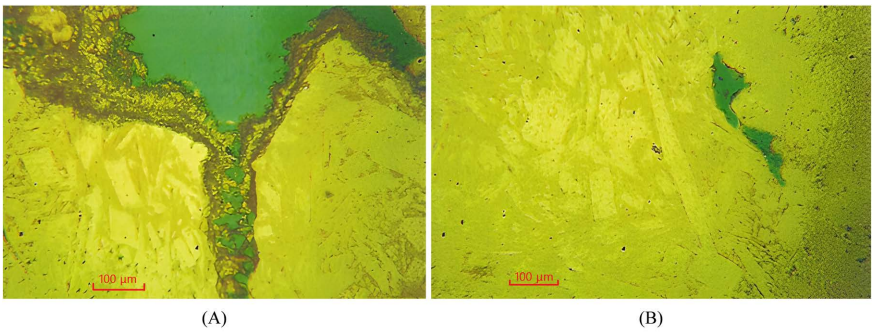

Figure 13. Stalk-like pseudomorphs of β-cristobalite recrystallized from the α-modification and following transformation to chalcedony (β-quartz). Note carbonate "rim cement" precipitated along fissures during cooling down. Originally melted Kurnub sandstone recovered from the Central Uplift, Jebel Waqf as Suwwan, thin section, X-nicols [26].

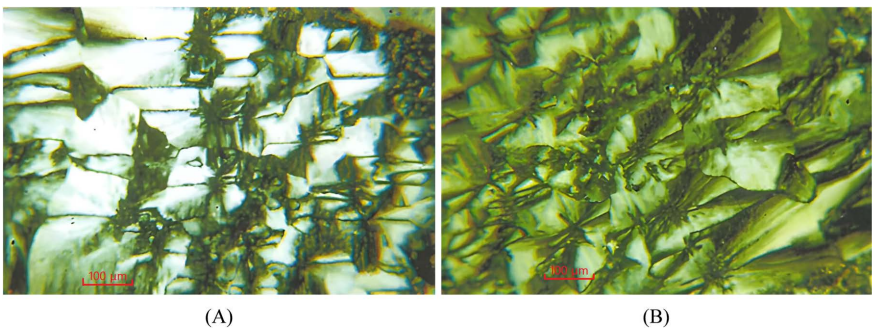

Figure 14. "Ballen structure" generated by the transformation of α-to β-cristobalite, result of volume reduction (~7%), following transformation to chalcedony. Originally melted Kurnub sandstone from the Central Uplift of Jebel Waqf as Suwwan, thin section, X-nicols [26].

pyroxenite-sanidinite facies conditions (1.100˚C), [25] [26], formerly mineralogically analysed in Israel [28]-[32]. Low and high temperature hornfels-facies of the marble exhibits a broad multicolored spectrum of deformation, loss of primary sedimentary structures, dikes, breccia, manifold hydrothermal travertine precipitation, chaotic post-deformation carbonate clastics (**Figure 15**), originally interpreted as products of self-combustion of the bituminous deposits [33]. However, during our revisit of Jizha site (26) we encountered, in connection with other impact-suspicious sites (**Figure 1**), a feature assemblage that indicates an Impact-Ricochet-track (Downrange "Fireline" = Avenue of Thermo-cataclysm across Jordan [27].

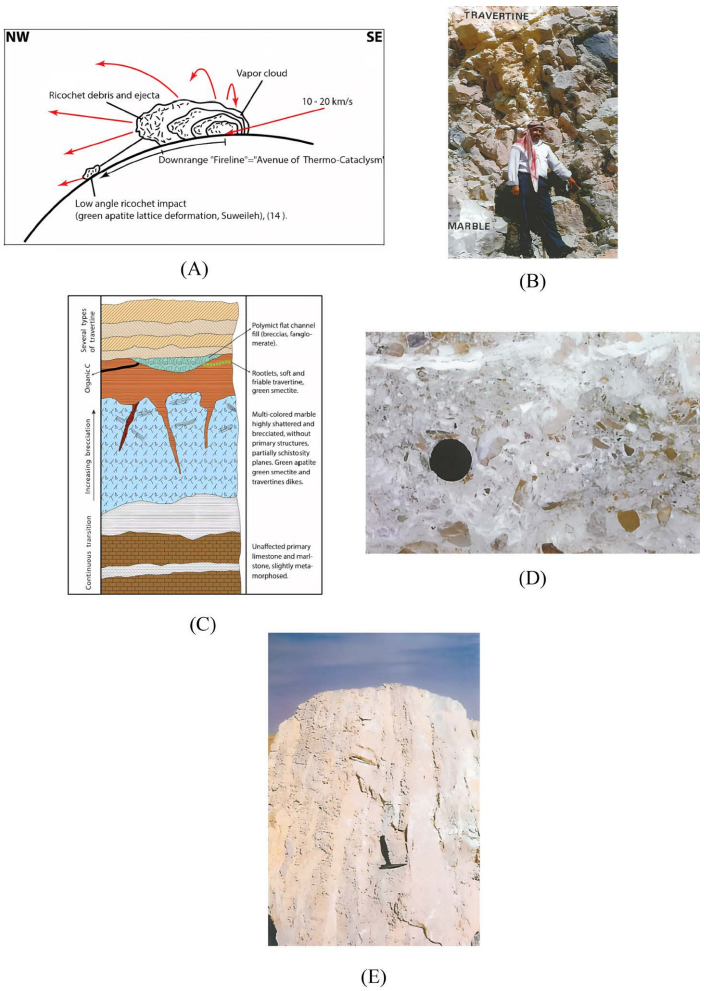

Figure 15. Jizha quarry located on the Ricochet track, ~35 km SE Amman: (A) Model of ejecta and whirlstorm effects (~1800˚C) after an oblique impact [27] applied to the Thermo-Cataclysm track across Jordan. (B) Multicolored, highly brecciated marble of Sanidine-Hornfels Facies penetrated and overlain with hydrothermal travertine, part of the "Mottled Zone" [26]. (C) Schematic section of high temperature marble overlain with bedded low temperature travertine [26]. (D) Poorly sorted calcareous resediments intercalated in bedded travertine; note fried surface of pebbles (arrows), [26]. (E) Vertical travertine dikes consisting of several precipitation phases cutting through brecciated marble of Sanidine-Hornfels Facies caused by ascending hot groundwater [26].

3. Results and Discussion

A) The Impact-Ricochet-Ensemble across the Jordanian Platform

All relevant structures own the same stratigraphic position and target area-lithology through the Eocene-Oligocene Transition, briefly characterized as follows:

- Jebel Waqf as Suwwan impact crater, E Jordan, N 31˚02.9', E 36˚48.4' (**Figure 16**), ~6 km Ø, Central Uplift (~1 km Ø), ring structure. Shock indicators: shatter cones, PDF in quartz grains, carbonate-chert agglomerate ("impact chess square"), recrystallized SiO_2 glass bombs showing fluidal textures (chert, siliciclastics), retrograde transformation: melt → cristobalite → tridymite → quartz, positive gravity anomaly [13] [15] [22]-[24] [26] [34].
- Ring Structure Wadi el Murbak, Iraq/Jordan border, N 32˚44'48"/E 39˚00'39", (**Figure 17**), ~7.5 km Ø, central uplift (2.5 km Ø), inner and outer ring, breccias drilled without petrographic data, hitherto no mineralogic shock indicators, arcuate structures in its western foreland [26] [28] [29] [34] [35].
- Al Umchaimin Crater, W Iraq, Wadi Walai, N 32˚35'07", E 39˚25'07.6", (**Figure 18**), ~3.3 km Ø. without central uplift, depth 23 - 28 m, arcuate fault inside the crater and arcuate structures in its western (Jordanian) foreland (**Figure 18**), crater rim impressively marked by a basaltic girdle, no basalt outflow, however strewnfields of basaltic boulders scattered in the foreland up to 20 km distance, crater located on a SW-NE running fault, hitherto no reliable mineralogic shock indicators [26] [36]
- Major Crater ("Caldera"?, NW Saudi Arabia, 100 km SW Jebel Aneiza, N 31˚13'57.35", E 38˚38'22.14", elev. 790 m, ~60 km Ø, satellite image, Google Earth, 2010, depth 125 - 160 m (**Figure 19**), arcuate fault along 8 km at NW-crater rim, radial drainage towards the basalt central cone exposing radial outflows, lava-capped crater rim, comp. UAC! [26] [30] [36].

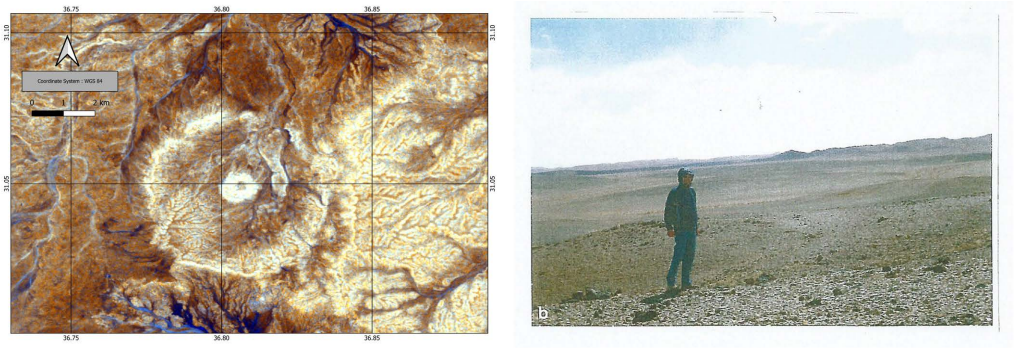

(A) (B)

Figure 16. (A) Impact crater Jebel Waqf as Suwwan (~7 km Ø), E Jordan exposing Central Uplift (~1 km Ø), inner and outer rim. Eocene escarpment on the eastern side. The Wadi's drainage system inside and outside the structure reveals the morphology [13], Hunting Techn. Serv., Ltd. London, 1956). (B) Note: small late-comer impact between Central Uplift and Outer Ring. Impact time-span may comprise the interval 34.0 - 33.9 Ma (~100 kyr) in close relation to B1 - B3-outpouring; Eocene Escarpment in the E background.

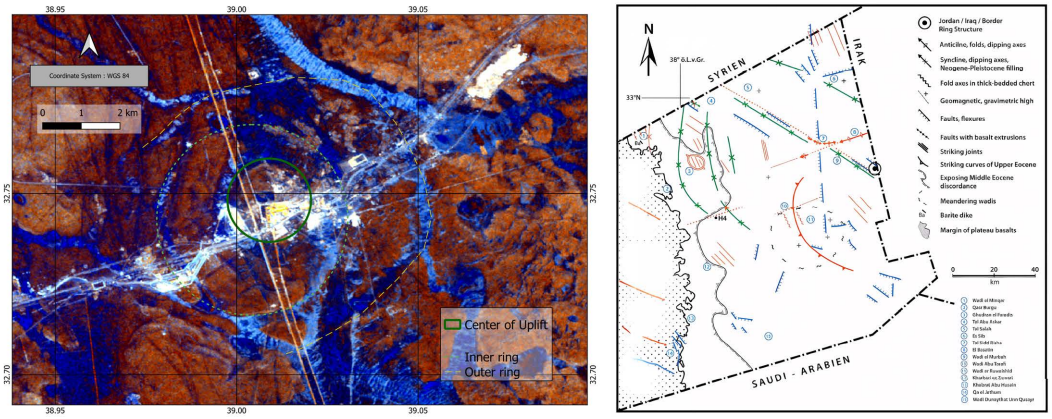

(A) (B)

Figure 17. (A) Aerial photograph of the Jordan-Iraq Ring Structure (7.5 km Ø) Wadi El Murbak (WEM): Central uplift (basalt?), inner and outer ring: Eocene carbonate rocks, chert, in-between arcuate wadis filled with clastic sediments [15] [35]; Hunting Techn. Serv., Ltd., London, Range Classification Survey of the H.K. Jordan, unpubl. Report, 40 p., 1956. (B) Arcuate striking curves of the Eocene and anticlines/synclines obviously relating to both impacts AUC and WEM located east of the B4-outpourings [15].

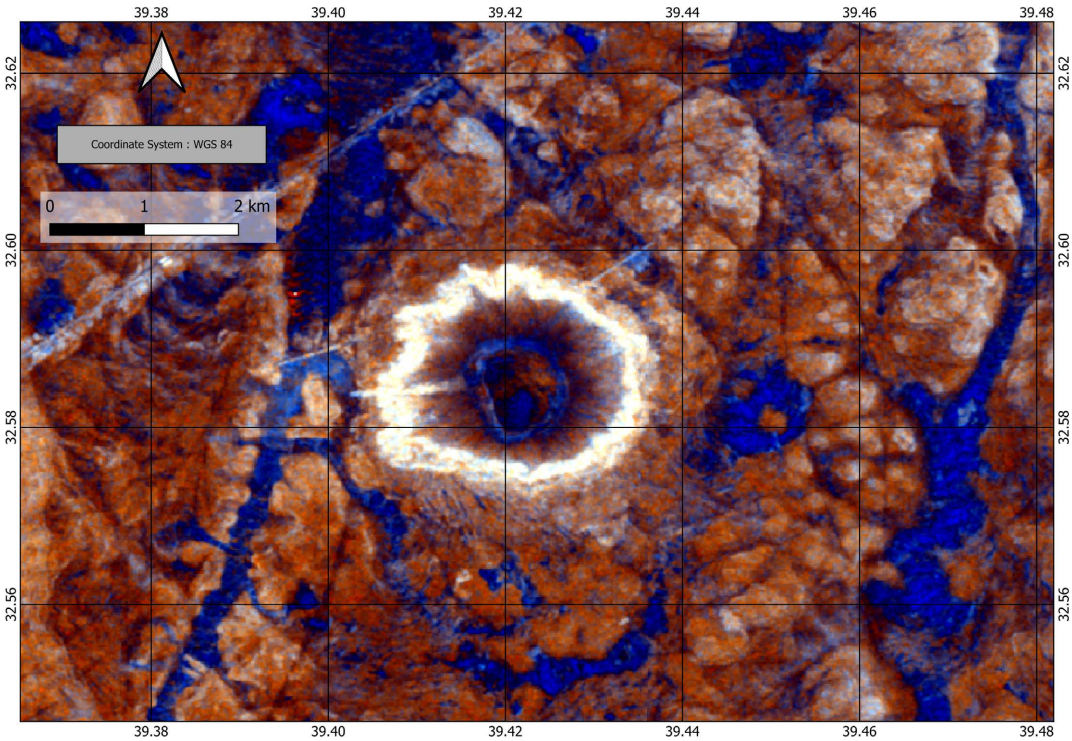

Figure 18. Al Umchaimin Crater (AUC), W Iraq (2 km Ø), drainage of wadis along radial faults decorated by Fe_2O_3- mineralization, mud flats in center, basalt seam along crater rim, lithostratigraphy see **Figure 5**, outer ring partially penetrated with basalt?, identic with B1 - B3? [36]. Note: circular basalt rimmed structures (~some 100 m Ø), not completed effusions = "burried harrats?).

- Zakimat al Hasa, SE Jordan, NE (**Figure 20**), asymmetric oval anticline (~1.3 × 2.5 km) along a SW-NE striking fault, ~120 m uplift of Kurnub sandstone, baryte cementation, hitherto without shock indicators, however, to be ex-

pected (shatter cones, PDF) [16] [26].

- W-margin of Baqa'a Basin, ~10 km NW of Amman, NE (**Figure 21**), transpressive flexure along a NW-striking fault, uplifted Kurnub sandstone [25] [26] [37], complete Late Cretaceous sequence comprising ~8 m Maastrichtian phosphorite: thermoclastic deformation to green apatite, multicolored "mottled" limestone, comp. similar occurrences at Qasr al Hammam, Dabaa, Al Qatrana, no reliable impact features [25] [26] [37].
- Centroclinal structure ~25 km SSW Jebel as Safra, between Qasr Tuba and Qasr Kharana (T-K), (**Figure 22(A)**), centroclinal strike of anticlines and synclines (relics of ring structures?), [13] [16] [25], ~15 km Ø; central uplift of Kurnub sandstone.
- Suspicious ring structures like T-K located between Dahikiya and pump station H5 (D-H 5), ~40 km Ø, uplift of two Kurnub—"blocks", arcuate wadis [13] [16] [25], (**Figure 22(B)**).
- Jizha Quarry, ~25 km SW of Amman, N 31˚70'115, E 35˚98' 300 (**Figure 15**), thermocataclysm of Maastrichtian-Danian bituminous carbonate rocks to marble, multicolored, brecciated, without primary sedimentary structures, hornfels-facies, green apatite and montmorillonite (comp. WMB), opal C-T [38], several travertine facies types filling dikes, joints and ponds caused by groundwater eruptions and post-ricochet reworking (polymict breccia) [26].

B) Corresponding Driving Forces and Effects through the Eocene-Oligocene Transition With Plate Tectonic Background

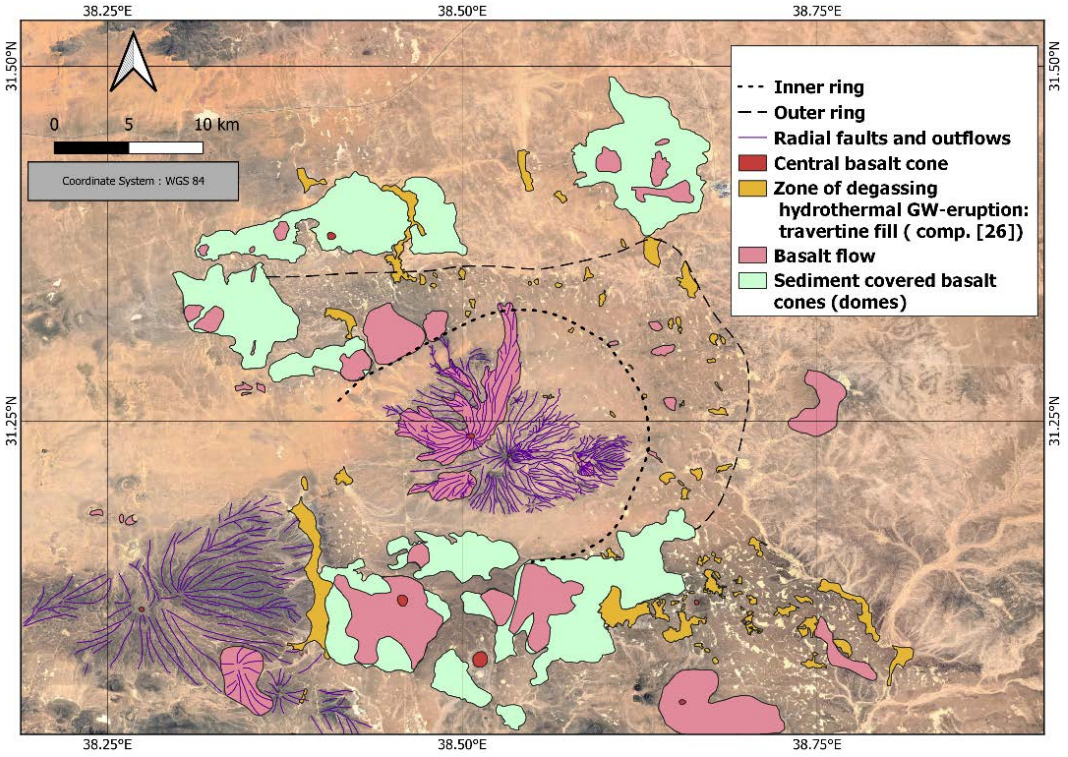

(A)

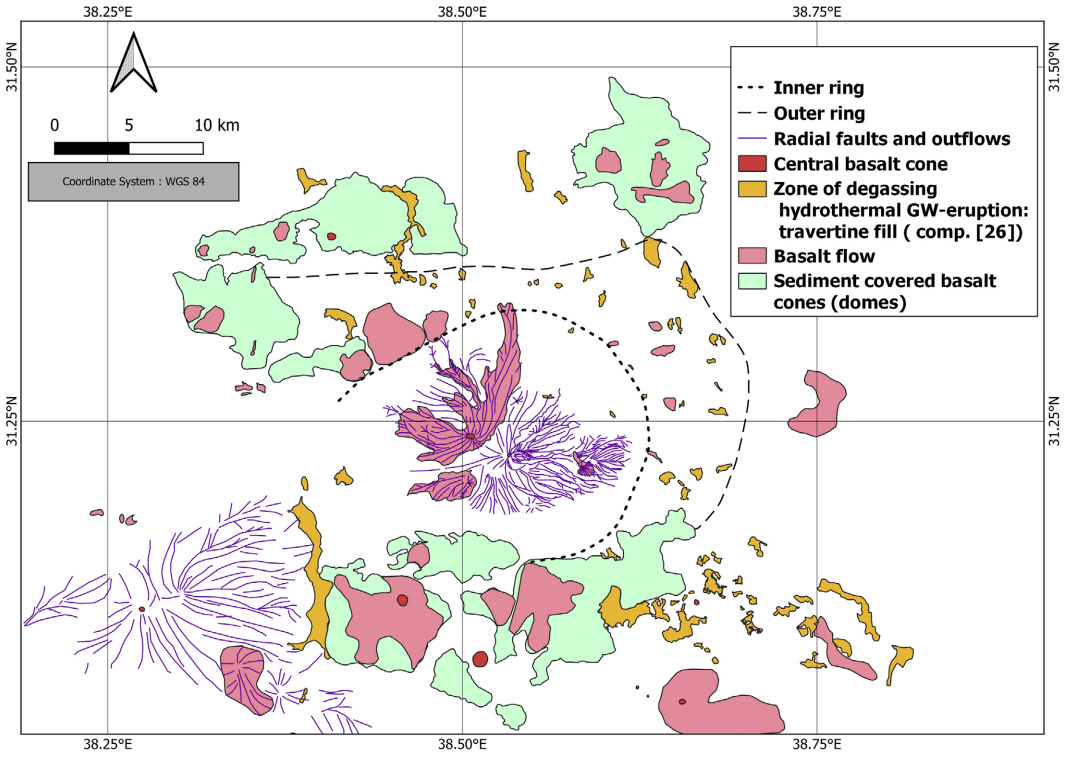

(B)

Figure 19. A, B: Satelite Image, Google Earth, 2010. Questionable major crater (CC), NW Saudi Arabia, coordin. see above. ~60 km Ø, depth 125 - 160 m, (B) represents a sketch map redrawn from (A). It exhibits a kind of a central uplift with a basaltic cone and radial outflows; outward follows a sand-covered ring-like syncline confined by a ring of circular arranged caps of basalt cones and highly disturbed sedimentary target rocks (probably Maastrichtian to Middle Eocene). This zone is characterized by innumerable circular and angular patches/pipes, which may be interpreted as effects of high pressure degassing and hydrothermal groundwater eruptions, later masked by mud flats: a result of impact that triggered the melt ascent. (see Jizha site and [26]). The preferred NNE-striking of the pipes and the three extremely elongated joints/fractures? meet the general NW/NNW-striking fault system dominating the Arabian Shield [9] [19]. The westward opening of the crater may indicate Ricochet erosion.

The Neogene plate tectonic scenery of the Near-Middle East comprises the initial opening of the Red Sea [9] [8] [19], the Dead Sea-Jordan Valley rifting [13] [20], the Miocene upheaval of the Arabien Shield [9] [18] [21], NW-directed faulting/plateau basalt outpourings [9] [13] [14] [19] and the collision of the Arabian Plate with the Eurasian Plates [39].

However, precursers of the Jordan Valley rifting took place during Late Cretaceous caused by transpressive/transtensional strike slip tectonics that directed regional lithofacies change by the formation of basins and swells across the Jordanian Platform [13] [40].

Of special interest appears the Azraq-Sirhan structure [9] [19] [41] running along the Jordanian-Saudi Arabian border, presenting a Paleocene to Miocene succession of marine sediments and marginal fanglomerate deposits immediately west of the Harrat Shamah plateau basalt (**Figure 1** and **Figure 6**). It may exhibit a fault-bounded seaway from the Indic Ocean to the Tethys via NE Jordan based

on crustal attenuation and a "failed Red Sea spreading" by encratonic rifting (comp. [42], (**Figure 23(D)**).

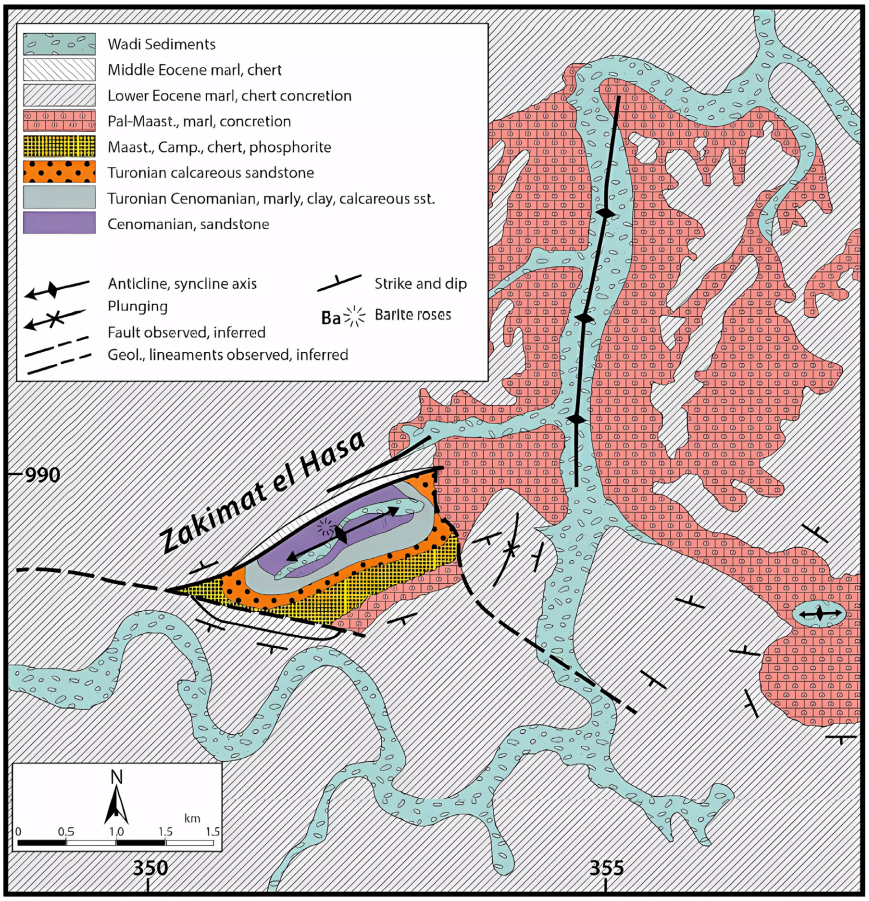

Figure 20. The oval anticline of Zakimat Al Hasa (ZAM), Central Jordan [15] [26] [34]. Note baryte cement in the Kurnub sandstone, ~120 m uplifted along a NE-running fault.

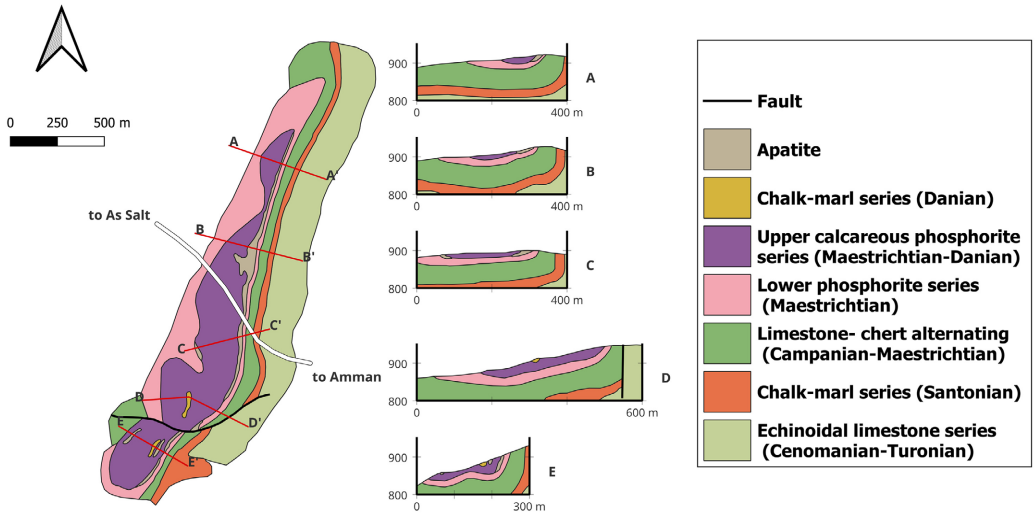

Figure 21. Transpressive asymetric flexure Suweileh/Baqa'a (SB) with uplifted Kurnub sandstone, ~8 m Maastrichtian phosphorite transformed to green apatite (~900˚C), multicolored "Mottled Limestone" [25]-[27].

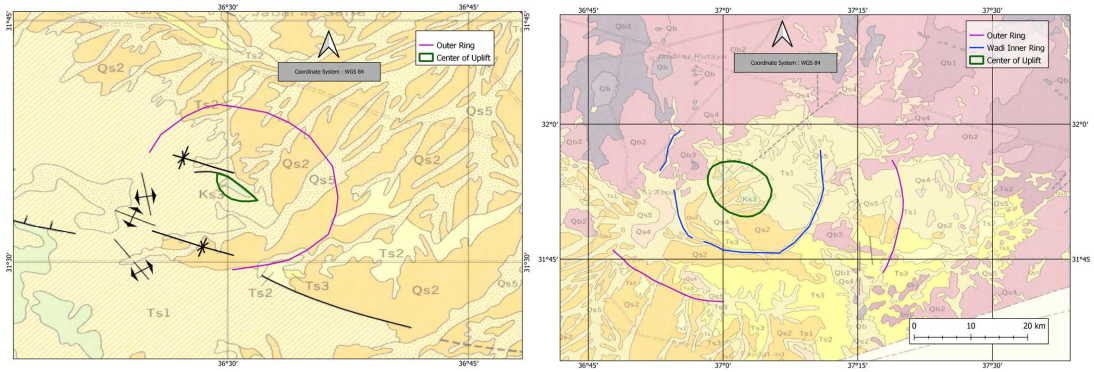

(A) (B)

Figure 22. Impact suspicious structures (A) Ringstructure located between Qasr Tuba and Qasr Kharana (T-KH), centroclinal striking of anticlines and synclines, Kurnub sandstone as central uplift?, ~15 km Ø [15] [16] [25]. (B) Ring structure? like (A), located between Dahikiya and pump station H5 (D-H 5), ~40 km Ø, uplift of Kurnub sandstone, arcuate wadis [13] [16] [25].

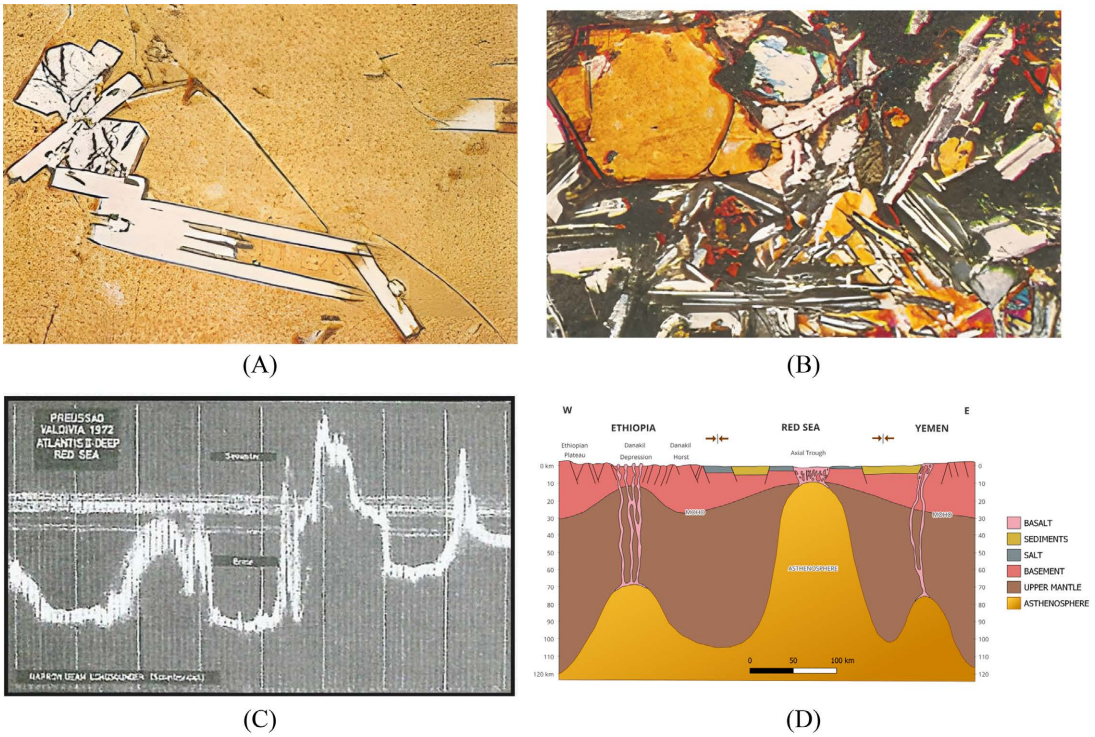

(A) (B)

(C) (D)

Figure 23. Red Sea Rifting ([9] [18] [19]. (A) Holocrystalline olivine-tholeiitic basalt from outside the Central Graben: Olivine, plagioclas, pyroxene. (B) Alkalibasaltic rock glass, phenocrysts of olivine and plagioclas (not in equilibrium with melt! Atlantis II Deep. (C) Cross-section shows the asthenolite undulation between Ethiopia-Red Sea-Yemen. In continuation of the latter: Saudi Arabian Harrats and the Azraq-Sirhan Basin.

Tholeiitic intrusions (dike, sill) indicate the true Red Sea rifting on ~41.8, 40.7 and 33.7 Ma [9], (**Figure 23**); obviously, the Lutetian-Bartonian unconformity (**Figure 5**) relates to it.

The Saudi Arabian "Harrat" magmatism presents olivine-basalt, alkali-olivine basalt and a few derivates [9] [19], based on partial melting of garnet-peridotite in

the asthenosphere (~100 km depth), accumulated in the crust-mantle boundary (~33 - 44 km depth) by ascent along NNW-running linear fault systems parallel to elongated basins like Wadi Azraq as Sirhan and combined with the Miocene upheaval of the Afro-Arabian Dome. Table 1 lists up the petrochemical composition of the volcanic rocks of Saudi Arabia, Red Sea and NE Jordan [9] [14] [18] [19].

The Red Sea-VALDIVIA-Cruise 3 [18] provided volcanic samples from the axial trough (Atlantis II-Deep) like olivine-basalts, rock glass without modal pyroxene caused by rapid magma ascent from the asthenosphere (8 km depth) without differentiation (Figure 23(A)-(C)) while outside the central trough holocrystalline alkali-basalt, olivine tholeiitic basalt, hyaloclastite and tuff indicate some crustal residence (Figure 23(D)).

Table 1. Major Elements of Cenozoic Plateau Basalts of the Arabian Nubian Shield: 1: VS-45, Seamount, Red Sea: 2, V-5, Atlantis II-Deep Red Sea, 3: V-22 Central Trough, Red Sea [18], 4: V-53, marginal Central Trough, Rea Sea, 5: NE Jordan, average [14], 6: Harrat Rakhat, 7: Harrat Kura and Khanbar, Saudi Arabia [9] [19], in %.

	1	2	3	4	5	6	7
SiO_2	46.4	49.6	50.3	49.6	45.97	48.03	48.54
Al_2O_3	14.2	14.8	14.1	18.5	14.60	16.04	16.76
Fe_2O_3	2.0	1.9	1.6	2.1	3.0	10.81	10.53
FeO	6.1	8.95	10.8	5.9	8.16		
MgO	7.9	7.3	7.1	5.1	8.58	9.02	8.28
CaO	11.7	12.4	11.3	12.5	10.48	10.88	11.12
Na_2O	3.2	2.5	2.3	2.8	4.02	2.90	2.94
K_2O	0.6	-	-	0.1	0.97	0.43	0.49
TiO_2	1.35	1.2	1.4	1.15	1.97	1.53	1.63
P_2O_5	0.31	0.14	0.17	0.19	0.37	0.20	0.21
MnO	0.16	0.21	0.23	0.15	0.23	0.17	0.17

The interplay of driving forces (impact, volcanism, tectonics) and resulting effects (climate, EOB-Lithofacies change, stepwise micro-fauval extinction, magma outpouring/degassing (B4, B7) and the impact-triggered $CaCO_3$, -dissoziation (~900˚C) find a satisfying interpretation by the $\delta^{13}C$- and $\delta^{18}O$- isotope excursions [11] (Figure 24).

However, since the skeletal carbonate preservation is restricted by partial dissolution (decreasing pH!) and poor in the GSSP at Massignano, Italy at the extinction level of Hantkeninida, there exists some uncertainty in connection with the global environmental change [11] [12] [16] [17]. Therefore, we use the time scale in [11] applied in the Kilwa Group of Tanzania Drilling Project (TDP: site [11] [12] [17] because of more detailed resolution of the isotope excursions through which results in a time-span difference of ~200 kyr for the EOB.

Throughout the interval of Late Cretaceous to uppermost Eocene (~72 - ~34

Ma) "Greenhouse"-conditions directed the lithofacies of the pelagic carbonate-chert deposits owning a stable plankton diversity (Shannon-Index: 2.4 - 2.8) intercalated by the Lutetian-Bartonian b. unconformity in NE Jordan meeting the subvolcanic Red Sea Rift-precursors [9] (**Figure 3**) (41.3 Ma).

The EOT (~34 - 33.5 Ma) covers 500 - 750 kyr (**Figure 24**). Its onset relates to the major impacts of Popigai, Chesapeake and others [4]-[6], possibly, slightly earlier than the Jordanian impact strewnfield/Ricochet track took place (**Figure 1**), accompanied by tremendous $C0_2$-degassing by $CaCO_3$-dissoziation (~900˚C), extinction of nannoplankton Discosaster Saipanensis because of photosynthesis stop at ~1.200 ppm CO_2 [43], (**Figure 25(A)**, **Figure 25 (B)**)-outpouring (see negative $\delta^{13}C$- and $\delta^{18}O$-excursions at ~34 Ma) (**Figure 24**).

Stepwise extinction of *Globigerina* Pella papillatum (~33.8 Ma), *Turborotalia* spp. (~33.75 Ma) and finally of Hantkeninidae [10]-[12] (~33.7 Ma = EOB) are accompanied by alternating $\delta^{18}O$ and $\delta^{13}C$-excursions caused by the basalt outpourings B_2, B_3 including degassing and intercalated paleosol formation and possible impact activity until the end of EOT (~33.5 Ma) (**Figure 4**, **Figure 5**, **Figure 24**).

According to **Figure 24(A)**, the Impact-Volcanic Interplay covered only the time span from 34.0 to 33.9 Ma (=100 kyr) while the time span between step 1 and step 2 (positive $\delta^{18}O$-excursions) may characterize continued outpouring and relating paleosol formation.

The lower EOT presents a period of ecologic disaster when the Late Eocene baryte-bearing bituminous marls correspond with impacting and B_1 - B_3 volcanism under oxygen-deficient conditions and hydro-exhalation baryte origin and lost photosynthesis ("Cosmic Winter").

The Early Oligocene Glacial Maximum (EOGM): (33.6 - 33.0 Ma) appears after Step 2 (EOIS). It is evidenced in Jordan (Dahikiya area, NE Azraq Basin) by glauconite-bearing siliciclastics and calcarenite indicating by glauconite (Fe^{2+}, Fe^{3+}) increasing Eh, overlying the E-0 unconformity (**Figure 5**) and accompanied by renewed occurrence of nanoplankton.

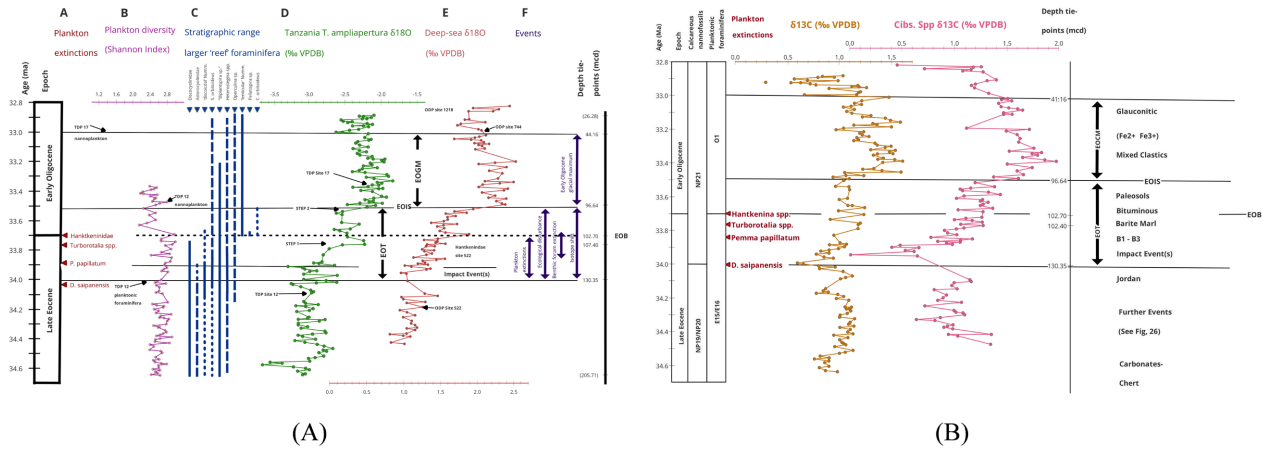

(A) (B)

Figure 24. $\delta^{18}O$- (A) and $\delta^{13}C$ isotope data (B) through the Eocene-/Oligocene transition (EOT), EOB: Eocene-Oligocene boundary, EOIS: maximum of $\delta^{18}O$ (step II), EOGM: Early Oligocene Glacial Maximum [11] [12].

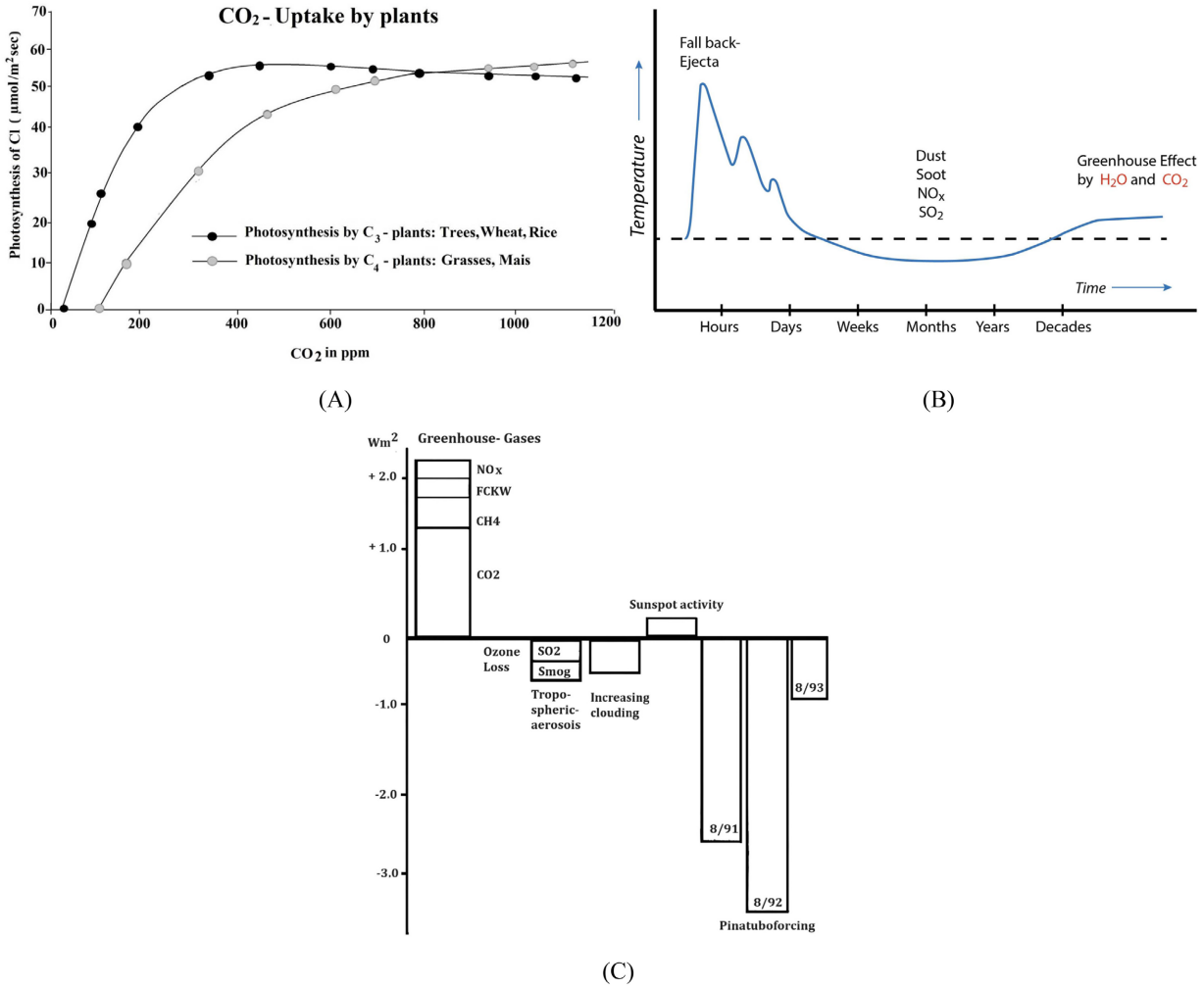

Figure 25. Effects of driving forces (A) Photosynthesis as a function of CO_2, [43] (B) Course of temperature after a major impact [44] (C) Climate forcing caused by both impacting and magmatism [40].

The Oligocene siliciclastics and mixed clastics are overlain, above the next unconformity, by the B_4-outpourings (**Figure 5**, **Figure 26**). According to (9, **Figure 3**), the latter meet coevally the initial Red Sea-volcanics (stage 1) in S Sinai during the uppermost Oligocene. The B4 plateau basalt of NE Jordan is again overlain with Lower Miocene calcareous, siliciclastics and sandy marls (~40 m: Al Azraq) during continued Red Sea-spreading. That mirrors the start of Miocene warming up and of the upheaval of the Afro-Nubian Shield during increasing heat flow and plate motion on global scale (Columbia River Plateau, Japan), [8].

C) Regulation of Lithofacies-Related Parameters (T, P, Ph, Eh, Gas Composition) Based on Climate-Forcing Impact and Volcanism Throughout the Eot.

For having the occasion to encounter a complex scenery (craters, tektites, ricochet track) of tremendous intensity in global scale (N America, Europe: Spain, Italy, Arabian Plate), one has to expect a triggering major cosmic event [2]-[5] [44] caused by a break-up of an asteroid (*i.e.* [45] or a comet from outside our solar system that crossed the Earth's orbit for fragmentation [46]-[49].

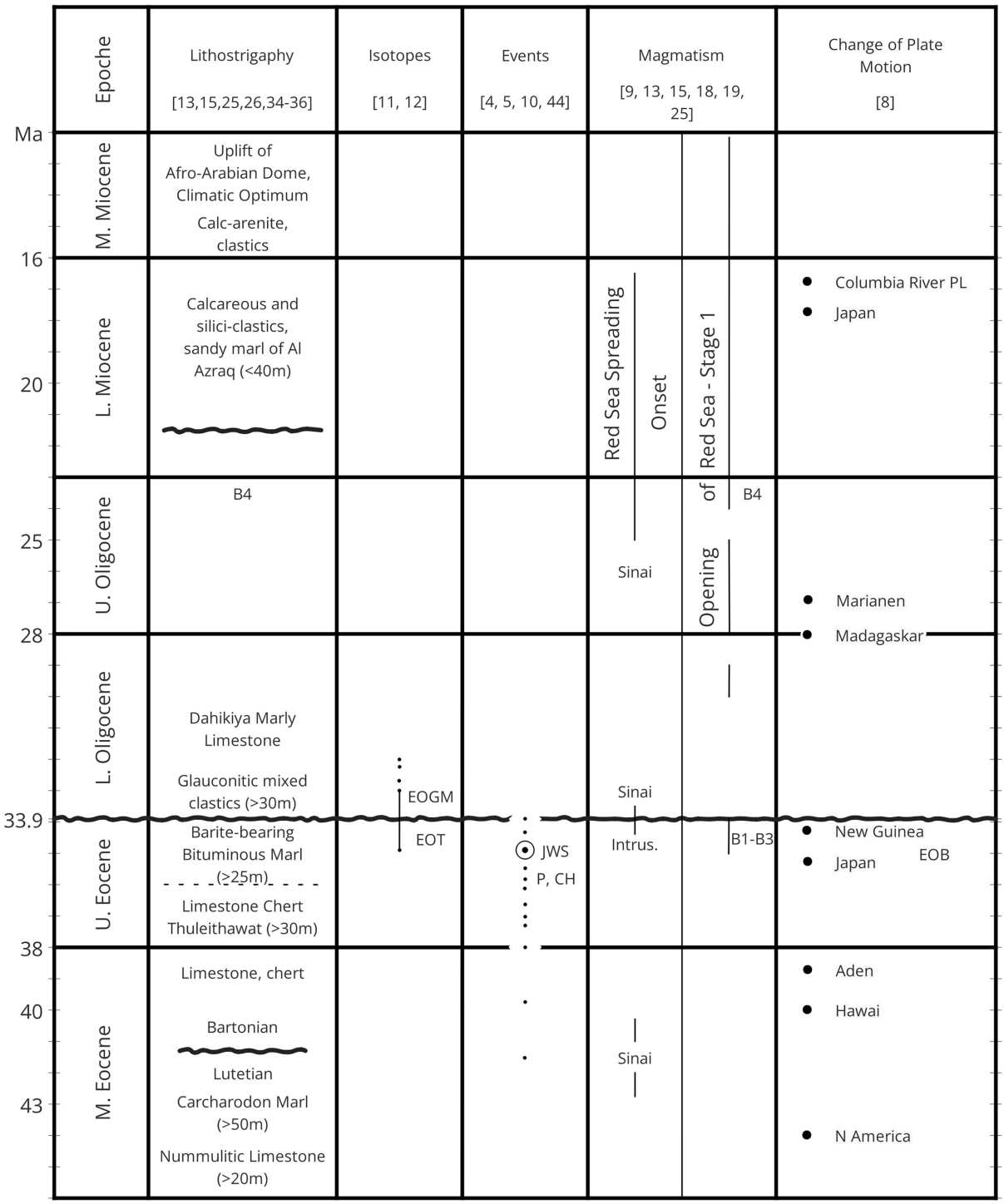

Figure 26. Event-stratigraphy through the middle eocene to middle miocene.

As an example, a L-chondrite (~200 km Ø) of the Main Asteroid Belt crossed the Earth's orbit ~470 Ma ago (M. Ordovician base) that caused through the next 8 Ma several minor meteorite impacts on the Fennoscandian Shield [45]: Lockne: (7.5 km Ø, Mälingen (0.7 km Ø), Kärdla, Granby, Tväreń/Baltica, and those of Ames, Clavin, Brent, Slate Island, Pilot; Meteorite falls: Kinnekulle,

Brunflo/Baltica (45); 3 - 5 Ma interval in average, in total: 470 - 445 Ma; recurrences accompanied by a velocity change of the Earth (10.73 → 12.26 km/Ma: [50], followed by worldwide subduction-related volcanic arc tephra-volcanism [51]: → K-bentonite).

Sequence-analytical and mineralogic data from the Ordovician of SE Jordan [52] reconfirm those from the Oslo site.

Another example for such a cosmic event caused by a giant comet, concerns the Pleistocene-Holocene Transition (~14.450 yr BP), [46]-[48] in coeval accompaniment with the significant end of the last glaciation and global tektite strewnfields [2] [3]: Indochinites, campbellites).

The recurrence of the smaller incoming comet every ~1.600 y and its possible collision with the Earth (~12.700 B.P. - 11.100 B.P. - 9.500 B.P. - 7.900 B.P. - 6.300 B.P. - 4.700 B.P, - 3.100 B.P. - 500 A.D. - 2.100 A.D.) has been brought in connection with events in the prehistorical/historical cultural evolution of Mankind related to the Near/Middle East and Europe [26] [48].

Returning to the EOT-scenery (34.0 - 33.5 Ma) on the Arabian Shield as an global Ensemble Member, Upper Eocene prominent impact precursors like Popigai and Chesapeake (~35.5 Ma) occurred when already a stepwise extinction of assimilating nannoplankton and planktonic foraminifers began and continued until the EOB (33.7 Ma; (**Figure 24**, **Figure 26**)).

However, a short interval of about 100 kyr (34.0 - 33.9 Ma) for the extinction of Discoaster saipenensis and 3 to 4 $\delta^{18}O$ and $\delta^{13}C$ excursions [10]-[12] (**Figure 24**, mirror both impacting and triggered basalt melt-outpouring [13]: (B1 - B3). These had led to the lithofacies change from carbonate-chert sequences to oxygen-deficient bituminous, baryte-bearing marl. Hence, documenting a decrease in pH, Eh and a dramatic increase in CO_2, caused by both volcanic degassing of exhalative origin and $CaCO_3$ dissociation (~900˚C) of the target rocks accompanied by loss of photosynthesis [43] **Figure 25(A)**). The result of this hazard left a period of ecologic distribution over an unconformity and including the formation of glauconite-bearing (Fe^{2+}-Fe^{3+}) mixed siliciclastics and calc-arenite during the Early Oligocene Glacial Maximum (EOGM) until ~33.0 Ma (**Figure 5**, **Figure 26**) under changing climate forces (**Figure 25(B)**, **Figure 25(C)**). Rising temperature (**Figure 25(B)**) led then to the deposition of mixed siliciclastic-carbonate sediments and recurrent microfauna.

Under plate tectonic aspects, the coeval evidence of both NW-trending fault systems [42] and attenuation of crustal thickness and subvolcanic intrusions (~34 Ma) in the S Sinai/Red Sea [9] as "failed" precursors of the Red Sea Rifting, together with the B1 - B3 effusions drilled at Wadi Zulayl (~34.0 - 33.9 Ma) are temporally connected to sills and dikes penetrating the basement of the Arabian Shield [42] up to a highstand magma level.

The impact structures located outside the post-Oligocene B4 - B6 plateau basalts (WEN, AUC, CC) that caused the B1 - B3-mobilization, however, exhibit thin basaltic seams and single basalt jets scattered as isolated blocks across their foreland (**Figure 18**), "burried harrats").

The AUC-crater tells that (comp. [36], magma, intruded along dikes and sills up to a surface-near level where it became reactivated by an impact just to decorate, by its insufficient volume, the crater walls/rims or to form irregular upwellings and domes in the Eocene sedimentary cover during B1 - B3-outpouring across the Wadi as Zulayl area (34 - 33.9 Ma).

The plateau basalts B4 - B6 of NE Jordan are part of the Shamah harrat, NW Saudi Arabia; they extruded along ~2.500 km from Yemen up to Syria after the Oligocene-Miocene boundary [9] [19] and are fully connected with the Red Sea-Opening since ~30 Ma.

4. Closing Remark

For a final reconfirmation, there is a need for K-Ar-radiometric ages from the B1 - B3 flood basalts and those of Wadi Al Umchaimin and the "Major Crater" (CC: ~60 km Ø), Saudi Arabia remains as a highly promising challenge for the Impact Community of the Near/Middle East.

The "symbiontic" Interplay of the parameters T, P. pH, Eh, gas composition doesn't only characterize the biological aspects of the GAIA-Principle [53] [54]; it also meets Geoscientific Processing as shown in this paper and in [41].

5. Conclusion

The current study reached the conclusion that: Local, regional, and worldwide interpretation and correlation of tectonic activities, volcanic eruptions, meteoritic impacts, climate changes, paleontological composition, species extinctions, mineral assemblages, sedimentary structures, and detailed rock-sequence analyses enhances the knowledge about the earth and the forces acting on it and the consequent implication on the earth system, in general, and on the local ontology in specific.

Acknowledgements

We are grateful to Kjell Paris for co-hunting "circular structures" on satellite photographs and to Olaf Schneider for digital work. Sincere thanks are also extended to Mohannad El Haj Yasseen (M. Sc.) for preparing the figures.

Conflicts of Interest

The authors declare no conflicts of interest regarding the publication of this paper.

References

[1] Schneider, W. and Salameh, E. (2018) How to Trace out Impact-Triggered Effects Globally Scattered around Formation Boundaries: Case Uhry, North Germany (Eocene/Oligocene Boundary). *Open Journal of Geology*, **8**, 9-32. https://doi.org/10.4236/ojg.2018.81002

[2] Barnes, V.E. (1963) Tektite Strewnfields. In: O'Keefe, A., Ed., *Tektites*, University Chicago Press, 25-50.

[3] Glass, B.P., Swincki, M.B., and Zwast, P.A. (1979) Australasian, Ivary Coast and N

American Tektite Strewnfields-Size, Masse and Correlation with Geomagnetic Reversals and Other Earth Events. *Proceedings of the* 10*th Lunar and Planetary Science Conference*, 19-23 March 1979, 2535-2245.

[4] Montanari, A. (1990) Geochronology of the Terminal Eocene Impacts; an Update. In: Sharpton, V.L. and Ward, P.D., Eds., *Geological Society of America Special Papers*, Geological Society of America, 607-616. https://doi.org/10.1130/spe247-p607

[5] Gehrels, T. (1994) Hazards Due to Comets and Asteroids. University Arizona Press.

[6] Ernstson, K. and Fiebag, J. (1992) The Azuara Impact Structure (Spain): New Insights from Geophysical and Geological Investigations. *Geologische Rundschau*, **81**, 403-427. https://doi.org/10.1007/bf01828607

[7] Zachos, J., Pagani, M., Sloan, L., Thomas, E. and Billups, K. (2001) Trends, Rhythms, and Aberrations in Global Climate 65 Ma to Present. *Science*, **292**, 686-693. https://doi.org/10.1126/science.1059412

[8] Price, N.J. (2001) Major Impacts and Plate Tectonics. Routledge. https://doi.org/10.1201/9780203165454

[9] Camp, V.E. and Roobol, M.J. (1989) The Arabian Continental Alkali Basalt Province: Part I. Evolution of Harrat Rahat, Kingdom of Saudi Arabia. *Geological Society of America Bulletin*, **101**, 71-95. https://doi.org/10.1130/0016-7606(1989)101<0071:tacabp>2.3.co;2

[10] Keller, G. (1986) Stepwise Mass Extinctions and Impact Events: Late Eocene to Early Oligocene. *Marine Micropaleontology*, **10**, 267-293. https://doi.org/10.1016/0377-8398(86)90032-0

[11] Pearson, P.N., McMillan, I.K., Wade, B.S., Jones, T.D., Coxall, H.K., Bown, P.R., *et al.* (2008) Extinction and Environmental Change across the Eocene-Oligocene Boundary in Tanzania. *Geology*, **36**, 179-182. https://doi.org/10.1130/g24308a.1

[12] Hutchinson, D.K., Coxall, H.K., Lunt, D.J., Steinthorsdottir, M., de Boer, A.M., Baatsen, M., *et al.* (2021) The Eocene-Oligocene Transition: A Review of Marine and Terrestrial Proxy Data, Models and Model-Data Comparisons. *Climate of the Past*, **17**, 269-315. https://doi.org/10.5194/cp-17-269-2021

[13] Bender, F. (1975) Geology of the Arabian Peninsula, Jordan. Professional Paper, United States Geological Survey.

[14] Boom van den, G. (1968) Zur Petrogenese der Plateaubasalte NE-Jordaniens. *Geologisches Jahrbuch der BGR*, **85**, 489-496.

[15] Heimbach, W. (1970) Zur Geologie NE-Jordaniens. *Geologisches Jahrbuch der BGR*, **88**, 265-288.

[16] Gradstein, F.M., Ogg, J G., Schmitz, M. and Ogg, G. (2012) The Geologic Time Scale. Elsevier.

[17] Cande, S.C. and Kent, D.V. (1995) Revised Calibration of the Geomagnetic Polarity Timescale for the Late Cretaceous and Cenozoic. *Journal of Geophysical Research: Solid Earth*, **100**, 6093-6095. https://doi.org/10.1029/94jb03098

[18] Schneider, W. and Wachendorf, H. (1973) Vulkanismus und Graben-Bildung im Roten Meer. *Geologische Rundschau*, **62**, 754-773. https://doi.org/10.1007/bf01820959

[19] Camp, V.E., Roobol, M.J. and Hooper, P.R. (1991) The Arabian Continental Alkali Basalt Province: Part II. Evolution of Harrats Khaybar, Ithnayn, and Kura, Kingdom of Saudi Arabia. *Geological Society of America Bulletin*, **103**, 363-391. https://doi.org/10.1130/0016-7606(1991)103<0363:tacabp>2.3.co;2

[20] Al-Zoubi, A.S. and Abu-Hamatteh, Z.S.H. (2009) Geological Evolution of the Jordan Valley. *Journal of the Virtual Explorer*, **32**, 1-9.

https://doi.org/10.3809/jvirtex.2009.00248

[21] Haq, B.U. and Al-Qahtani, A.M. (2005) Phanerozoic Cycles of Sea-Level Change on the Arabian Platform. *GeoArabia*, **10**, 127-160. https://doi.org/10.2113/geoarabia1002127

[22] Salameh, E., Khoury, H. and Schneider, W. (2006) Jebel Wagf as Suwwan, Jordan: A Possible Impact Crater a First Approach. *Zeitschrift der Deutschen Gesellschaft für Geowissenschaften*, **157**, 319-325. https://doi.org/10.1127/1860-1804/2006/0157-0319

[23] Salameh, E., Khoury, H., Reimold, W.U. and Schneider, W. (2008) The First Large Meteorite Impact Structure Discovered in the Middle East: Jebel Waqf as Suwwan, Jordan. *Meteoritics & Planetary Science*, **43**, 1681-1690. https://doi.org/10.1111/j.1945-5100.2008.tb00636.x

[24] Kenkmann, T., Reimold, W.U., Khirfan, M., Salameh, E., Khoury, H. and Konsul, K. (2010) The Complex Impact Crater Jebel Waqf as Suwwan in Jordan: Effects of Target Heterogeneity and Impact Obliquity on Central Uplift Formation. In: Gibson, R.L., Reimold, W.U., Eds., *Large Meteorite Impacts and Planetary Evolution IV*, Geological Society of America, 471-487. https://doi.org/10.1130/2010.2465(23)

[25] Heimbach, W. and Rösch, H. (1980) Die "Mottled Zone" in Zentraljordanien. *Geologisches Jahrbuch der BGR*, **40**, 3-17.

[26] Schneider, W. and Salameh, E. (2014) Uncommon and Impact-Suspicious Geologic Phenomena across Jordan and Adjacent Areas, Arabian Plate. *Open Journal of Geology*, **4**, 680-717. https://doi.org/10.4236/ojg.2014.412051

[27] Schultz, P.H. and Gault, D.E. (1990) Prolonged Global Catastrophes from Oblique Impacts. In: Sharpton, V.L. and Ward, P.D., Eds., *Geological Society of America Special Papers*, Geological Society of America, 239-262. https://doi.org/10.1130/spe247-p239

[28] Bentor, Y.K., Gross, S. and Kolodny, Y. (1972) New Evidence on the Origin of the High-Temperature Mineral Assemblage of the "Mottled Zone" (Israel). 24th International Geological Congress, Section 2, 267-275.

[29] Gross, S. (1970) Mineralogy of the "Mottled Zone" Complex in Israel. List of Minerals. *Israel Journal of Earth Sciences*, **19**, 211-216.

[30] Gross, S. (1977) The Mineralogy of the Hatrurim Formation. Israel. The Mineralogy of the the Hatrurim Formation, Israel, Geological Survey of Israel.

[31] Kolodny, Y., Bar, M. and Sass, E. (1971) Fission Track Age of the Mottled Zone Event' in Israel. *Earth and Planetary Science Letters*, **11**, 269-272. https://doi.org/10.1016/0012-821x(71)90178-6

[32] Kolodny, Y., Schulman, N. and Gross, S. (1973) Hazeva Formation Sediments Affected by the "Mottled Zone" Event. *Israel Journal of Earth Sciences*, **22**, 185-193.

[33] Kolodny, Y. and Gross, S. (1974) Thermal Metamorphism by Combustion of Organic Matter: Isotopic and Petrological Evidence. *The Journal of Geology*, **82**, 489-506. https://doi.org/10.1086/627995

[34] Heimbach, W. (1969) Vulkanogene Erscheinungen in der Kalktafel Zentraljordaniens. Beih. *Geologisches Jahrbuch der BGR*, **81**, 149-160.

[35] Master, S. (2009) A Possible 7.5 km-Diameter Buried Impact Structure on the Jordan-Iraq Border: Geological Setting and Remote Sensing. *The First Arab Impact Cratering and Astrogeology Conference*, Amman, 9-11 November 2009, 58-60.

[36] Mitchel, R. (1958) The Al Umchamin Crater, W Iraq. *The Geographical Journal*, **124**, 578-580.

[37] Wiesemann, G. and Rösch, H. (1969) Zur Tektonik des Gebietes östlich des Grabenabschnittes Totes Meer-Jordantal. Beih. *Geologisches Jahrbuch der BGR*, **81**, 177-214.

[38] Khoury, H., Salameh, E., Schneider, W. and Khirfan, M. (2009) Chert from Jebel Waqf as Suwwan. The First Arab Impact Cratering and Astrogeology Conference, Amman, 9-11 November 2009, 42-44.

[39] Frisch, W. and Meschede, M. (2009) Plattentektonik. 3rd Edition, Buch-gesellschaft.

[40] Schmincke, H.U. (2000) Vulkanismus. Buch-gesellschaft.

[41] Schneider, W. and Salameh, E. (2024) Cretaceous Large Igneous Provinces (LIPs) Affect Sedimentary Processing: Jordan, Arabian Plate; NW Germany, Central Europe. *Open Journal of Geology*, **14**, 671-704. https://doi.org/10.4236/ojg.2024.146029

[42] Coleman, R.G., Fleck, R.J., Hedge, C.E. and Ghent, E.D. (1977) The Volcanic Rocks of SW Saudi Arabia and the Opening of the Red Sea. In: Directorate General of Mineral Resources, Ed., *Red Sea Research* 1970-1975: *Saudi Arabian Directorate General of Mineral Resources Bulletin* 22, Directorate General of Mineral Resources, D1-D30.

[43] Vahrenholt, F. and Lüning, S. (2021) Unerwünschte Wahrheiten, IMV. 6th Edition, Langen Müller Verlag

[44] Stöffler, D. (2002) Bedrohung aus dem Weltall. Asteroiden und Kometen. In: Emmermann, R., *et al*. Eds., *An den Fronten der Forschung. Verh*, Gesellschaft Deutscher Naturforscher und Ärzte (GDNÄ), 81-98.

[45] Ormö, J., Sturkell, E., Alwmark, C. and Melosh, J. (2014) First Known Terrestrial Impact of a Binary Asteroid from a Main Belt Breakup Event. *Scientific Reports*, **4**, Article No. 3724. https://doi.org/10.1038/srep06724

[46] Clube, V. and Napier, B. (1990) The Cosmic Winter. Blackwell.

[47] Clube, S.V.M. and Napier, W.N. (1986) Giant Comets and Galaxy. Implications of the Terrestrial Record. In: Smoluchowsky, J.N., *et al*. Eds., *The Galaxy and Solar System*, University Arizona Press, 260-285.

[48] Hoyle, F. (1993) The Origin of the Universe and the Origin of Religion. Moyer Bell.

[49] Wilkinson, D. (1991) Our Universes. Columbia University Press.

[50] Brink, H. (2006) Do the Global Geodynamic Cycles of the Phanerozoic Represent a Feedback System of the Earth and Is the Moon Involved as an Acting External Force? *Zeitschrift der Deutschen Gesellschaft für Geowissenschaften*, **157**, 17-40. https://doi.org/10.1127/1860-1804/2006/0157-0017

[51] Ballo, E.G., Augland, L.E., Hammer, Ø. and Svensen, H.H. (2019) A New Age Model for the Ordovician (Sandbian) K-Bentonites in Oslo, Norway. *Palaeogeography, Palaeoclimatology, Palaeoecology*, **520**, 203-213. https://doi.org/10.1016/j.palaeo.2019.01.016

[52] Schneider, W. and Salameh, E. (2024) Ordovician Sedimentary Processing and Relating Driving Forces: Jordan, Arabian Plate. Preprint.

[53] Lovelock, J. (1992) Gaia. Bern, München, Wien, Scherz. https://www.scirp.org/reference/referencespapers?referenceid=3758522

[54] Margulis, L. (1998) Symbiotic Planet. Basic Books.